Shock-induced $\mathcal{PT}$-symmetric potentials in gas-filled photonic-crystal fibers

Mohammed F. Saleh,[1] Andrea Marini,[1] and Fabio Biancalana[1,2]
[1]*Max Planck Institute for the Science of Light, Günther-Scharowsky Straße 1, 91058 Erlangen, Germany*
[2]*School of Engineering and Physical Sciences, Heriot-Watt University, EH14 4AS Edinburgh, United Kingdom*
(Received 29 October 2013; published 3 February 2014)

We have investigated the interaction between a strong soliton and a weak probe with certain configurations that allow optical trapping in gas-filled hollow-core photonic-crystal fibers in the presence of the shock effect. We have shown theoretically and numerically that the shock term can lead to an unbroken parity-time- ($\mathcal{PT}$-) symmetric potential in these kinds of fibers. Time irreversible behavior, a signature feature of the $\mathcal{PT}$ symmetry, is also demonstrated numerically. Our results will open different configurations and avenues for observing $\mathcal{PT}$-symmetry breaking in optical fibers, without the need to resort to complex optical systems.

DOI: 10.1103/PhysRevA.89.023801 PACS number(s): 42.65.Tg, 42.81.Dp

One of the postulates of ordinary quantum mechanics is that physical observables are associated with Hermitian operators, which are accompanied by a spectrum of real eigenvalues [1]. Surprisingly, Bender *et al*. found a class of non-Hermitian Hamiltonian operators that can also exhibit entirely real spectra, provided these operators satisfy the parity-time ($\mathcal{PT}$) symmetry [2,3]. Specifically, a Hamiltonian operator is said to be $\mathcal{PT}$ symmetric if $U(x) = U^*(-x)$, where U is the potential and x is the position. Therefore, the real part of the potential must be even, while its imaginary part should be odd. Interestingly, this class of operators is characterized by the existence of a certain threshold above which the $\mathcal{PT}$ symmetry is spontaneously broken and the entire spectrum of eigenvalues becomes complex. The $\mathcal{PT}$ symmetry has been investigated and explored theoretically [4–13] and demonstrated experimentally [14–17] in a number of different optical settings that exhibit gain and loss processes simultaneously. The structure complexity is the most common feature in these microstructures.

The invention of the hollow-core (HC) photonic-crystal fibers (PCFs) [18,19] presents a great opportunity to demonstrate the $\mathcal{PT}$ symmetry in the most successful waveguide of all, the optical fiber. Usually, the Raman nonlinear contribution is dominant in solid-core fibers and can cause this interesting phenomenon to deteriorate. However, HC PCFs based on a kagome lattice have extended the field of linear and nonlinear fiber optics well beyond the interaction of light with solid media [20]. A HC PCF can be filled with Raman-inactive gases such as noble gases, allowing unprecedented possibilities to study pure nonlinear effects without the disturbance of the Raman effect. In recent years, the study of HC PCFs filled with noble gases has led to the demonstration and prediction of interesting unexpected phenomena such as high harmonic generation [21], deep UV generation [22], soliton self-frequency blue shift [23–27], asymmetric self-phase modulation, and universal modulational instability [28].

In this paper we propose the HC PCF as an alternative structure in order to observe the $\mathcal{PT}$ symmetry in optics rather than using complicated microstructures with gain and loss that must be carefully balanced. Very recently, we introduced a system to observe optical trapping between two ultrashort pulses in HC PCFs filled by a noble gas due solely to the cross phase modulation (XPM) effect [29]. The system is Raman and plasma free. The two pulses have different scales of intensities: The strong pump pulse introduces a potential well that traps the weak probe pulse inside it. The two pulses must have the same frequency ω_0 to fulfill the group-velocity matching condition and different circular polarization states for a clear monitoring at the fiber output. In order to eliminate birefringence-induced coupling between the pulses, the fiber core should be perfectly symmetric. In this case, the propagation of the two pulses in a lossless medium are governed by the following set of normalized coupled partial differential equations [29,30]:

$$\begin{aligned} i\partial_\xi\psi_1 + \tfrac{1}{2}\partial_\tau^2\psi_1 + |\psi_1|^2\psi_1 + i\tau_{\rm sh}\partial_\tau(|\psi_1|^2\psi_1) = 0,\\ i\partial_\xi\psi_2 + \tfrac{1}{2}\partial_\tau^2\psi_2 + 2|\psi_1|^2\psi_2 + i2\tau_{\rm sh}\partial_\tau(|\psi_1|^2\psi_2) = 0, \end{aligned} \tag{1}$$

where ψ_1 and ψ_2 are the complex envelopes of the pump and the probe, respectively, ξ is the longitudinal coordinate along the fiber, τ is the time coordinate, and $\tau_{\rm sh}$ is the normalized self-steepening (shock) coefficient. The effect of higher-order dispersion coefficients and the nonlinearity of the probe are neglected. It is important to mention that the coupled equations in Ref. [30] do not include the shock term that is due to the frequency dependence of the nonlinear Kerr coefficient $\gamma(\omega)$. This effect can be included by first applying the Fourier transform on these equations via treating the nonlinear parts as constants, followed by expanding $\gamma(\omega)$ around ω_0 using the first-order Taylor series, and finally applying the inverse Fourier transform.

The governing equation of the propagation of the pump is found to be integrable and has a family of soliton solutions [31,32]. The fundamental solution has a form similar to the Schrödinger soliton, however, it is chirped,

$$\psi_1(\xi,\tau) = A\,\mathrm{sech}\theta\,\frac{B^* + 1 + (B^* - 1)\tanh\theta}{[B + 1 + (B - 1)\tanh\theta]^2}e^{iN^2\xi/2}, \tag{2}$$

where $\theta = N\tau$, $A = 2N(1 + N^2\tau_{\rm sh}^2)^{-1/4}$, $B = (1 + iN\tau_{\rm sh})A^2/4N^2$, and N is an arbitrary parameter that controls the amplitude and the width of the soliton simultaneously. The temporal and spectral profiles of the pump intensity are depicted in Figs. 1(a) and 1(b), respectively. It is clearly shown that the temporal dependence is symmetric, while the spectral dependence is asymmetric.

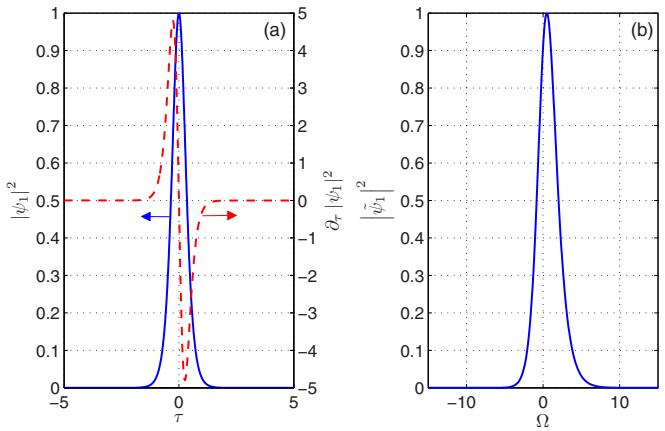

FIG. 1. (Color online) Solid blue curves represent (a) the temporal and (b) the spectral profile of the pump intensity, respectively. Here Ω is the normalized frequency shift, $N = 2.5$, and $\tau_{sh} = 0.1137$. These parameters are used in all the simulations shown in this paper, except in Fig. 2, where N is an independent variable. The time derivative of the temporal pulse intensity is shown by the dashed red curve in (a).

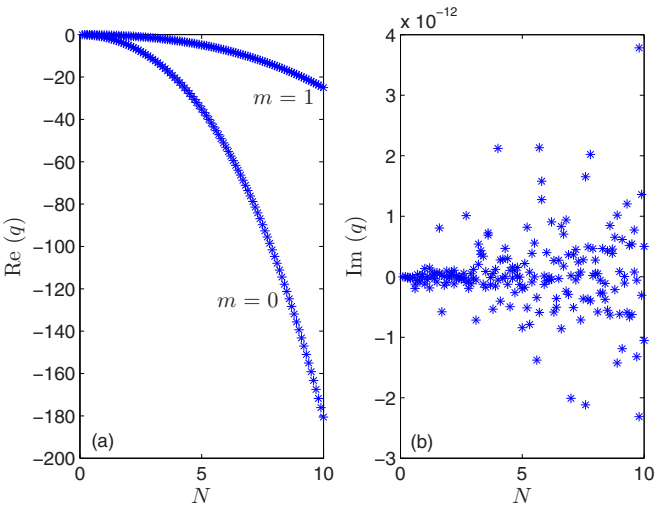

FIG. 2. (Color online) The N dependence of (a) the real and (b) the imaginary parts of the propagation constants of the probe in the fundamental $m = 0$ and the first-order $m = 1$ modes.

The probe propagates linearly since its nonlinearity is negligible. Its governing equation can be written as

$$i\partial_\xi\psi_2 + i2\tau_{sh}|\psi_1|^2\partial_\tau\psi_2 + \tfrac{1}{2}\partial_\tau^2\psi_2 + 2[|\psi_1|^2 + i\tau_{sh}\partial_\tau|\psi_1|^2]\psi_2 = 0. \quad (3)$$

Hence, the shock term introduces two terms proportional to τ_{sh}, as shown in Eq. (3). The first term results in additional time-dependent group velocity, while the second term modifies the trapping potential by an imaginary component. Introducing the phase transformation

$$\psi_2 = \tilde{\psi}\exp\left[-i2\tau_{sh}\int_{-\infty}^{\tau}|\psi_1(\tau')|^2 d\tau'\right], \quad (4)$$

Eq. (3) can be then simplified to

$$i\partial_\xi\tilde{\psi} + \tfrac{1}{2}\partial_\tau^2\tilde{\psi} + \left[2|\psi_1|^2 + 2\tau_{sh}^2|\psi_1|^4 + i\tau_{sh}\partial_\tau|\psi_1|^2\right]\tilde{\psi} = 0. \quad (5)$$

In seeking stationary solutions for the probe $\tilde{\psi}(\xi,\tau) = f(\tau)\exp(-iq\xi)$, with temporal profile f and propagation constant q, Eq. (5) becomes a linear Schrödinger equation in time

$$-\tfrac{1}{2}\partial_\tau^2 f + U(\tau)f = qf, \quad (6)$$

where $U = -2|\psi_1|^2 - 2\tau_{sh}^2|\psi_1|^4 - i\tau_{sh}\partial_\tau|\psi_1|^2$ is the potential well and q is the corresponding eigenvalue. This potential possesses a $\mathcal{PT}$ symmetry since its real part is even while its imaginary part is odd [see Fig. 1(a)]. Hence, the pump introduces a complex $\mathcal{PT}$-symmetric potential that affects the propagation of the probe. The real part of the potential traps the probe, while the imaginary part amplifies or attenuates the probe amplitude. In particular, the leading and trailing parts of the probe will experience loss and gain, respectively, with exactly the same magnitude. Note that such induced potential is only due to the XPM effect combined with the shock term, which is always important to consider for ultrashort pulses propagating in optical fibers. In addition, the phase structure of the soliton does not influence the form of the potential since U depends only on $|\psi_1|$.

This potential well has always two localized modes, similarly to the case where the shock coefficient is absent [29]. When the potential has the shape of a fundamental Schrödinger soliton, it can be easily demonstrated that the number of eigenvalues is constant and independent of the potential depth and width [1]. The reason for this unusual property is that the potential depth and width are exactly inversely related to each other in this case. In the presence of the self-steepening effect, we found numerically that this scenario still holds even for large physical values of τ_{sh}.

The localized modes can be computed numerically using the sparse matrix technique [33]. The real and the imaginary parts of the propagation constants are plotted versus the parameter N for both modes in Fig. 2. As shown, the values of the imaginary parts are negligible in comparison to the real parts and they follow a random distribution, which indicates that these values are just numerical errors. In other words, the propagation constants or the eigenvalues are always pure real values and there is no threshold for breaking the $\mathcal{PT}$ symmetry. In general, the real part of the potential tries to maintain the $\mathcal{PT}$ symmetry, while the imaginary part would be responsible for the breakup of this symmetry. In our case, the real part of the potential stays dominant in comparison to the imaginary part because the shock term affects both parts simultaneously with different powers of the parameter N. This result contradicts a general statement that a linear eigenvalue problem always has a zero threshold point or the $\mathcal{PT}$ symmetry in the corresponding system is always broken [6].

The proposed configuration does not allow a breaking of the $\mathcal{PT}$ symmetry, which would definitely be of considerable interest. However, it represents the foundation of an unconventional and relatively easily implemented scheme to realize the $\mathcal{PT}$-symmetric potentials in waveguides. The current

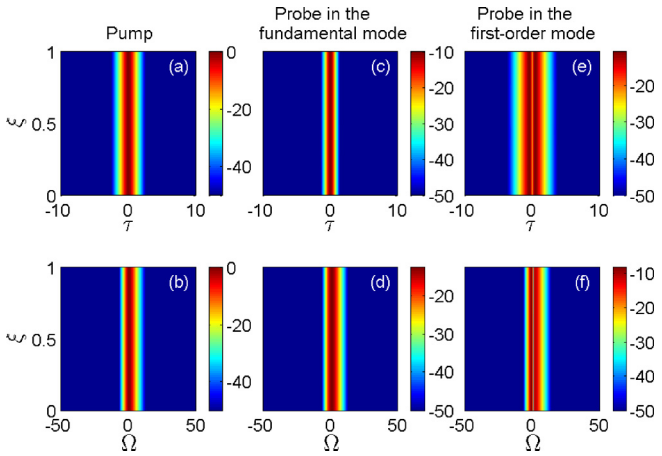

FIG. 3. (Color online) (a) Temporal and (b) spectral evolution of the pump. Temporal and spectral evolution of the copropagating probe, when it is in (c) and (d) the fundamental mode or (e) and (f) the first-order mode.

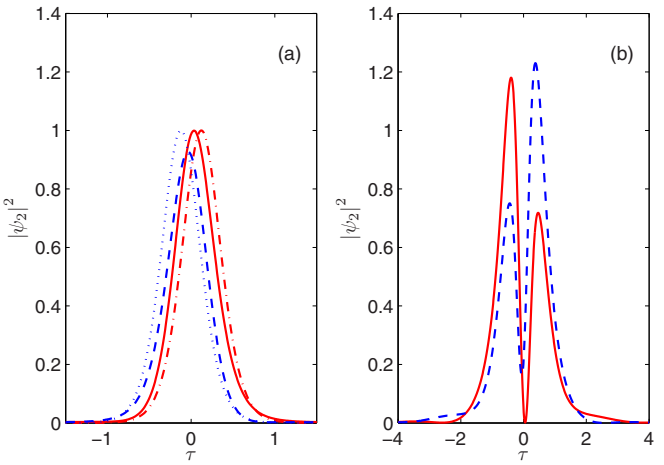

FIG. 4. (Color online) Temporal profiles of the probe at the fiber output, when it is launched in (a) the fundamental or (b) the first-order mode. Solid red and dashed blue curves represent the output profiles when the input probe is delayed with respect to the pump by $\Delta\tau = \pm 0.116$. Red dash-dotted and blue dotted curves in (a) represent the input probe, when it is delayed by $\Delta\tau = \pm 0.116$.

configuration is limited by the available free parameters, which are only the shock coefficient τ_{sh} and the parameter N. $\mathcal{PT}$-symmetry breaking will occur when the imaginary part of the pump-induced potential prevails over its real part. This can be achieved by seeking a challenging configuration with additional free parameters that can reduce or even eliminate the time-dependent group-velocity term in Eq. (3), which is responsible for the dominance of the real part of the potential in the current configuration.

The copropagation of the pump and the probe in either the fundamental or the first-order mode is shown in Fig. 3 by simulating Eq. (1). The probe does not suffer from dispersion-induced broadening during propagation due to XPM that traps the probe inside the soliton-induced potential. In designing a real physical system, the nonlinearity of the probe has also to be considered. After a certain propagation distance, the probe nonlinearity will start to affect not only its dynamics but the pump dynamics too. When this happens, the concept of the pump-induced trapping potential is no longer applicable. By increasing the ratio between the pump and the probe input amplitudes and designing the fiber length properly, this effect can be easily obviated.

$\mathcal{PT}$-symmetric waveguides are characterized by parity breaking even if the $\mathcal{PT}$ symmetry still holds, which is known in the literature as reciprocity breaking [16]. However, we prefer to use the term parity instead of reciprocity since the latter has caused a great deal of confusion that has been resolved recently [34,35]. The system is said to be reciprocal or nonreciprocal based only on the Lorentz reciprocity theorem. In the spatial domain, when one considers coupled $\mathcal{PT}$-symmetric waveguides, the light evolution is not the same when the beam is launched in one waveguide or the other because of this parity-breaking property. In the time domain, the parity and time-reversal operators exchange roles, hence, we expect an irreversible temporal behavior. By mimicking the same experiment in the time domain by introducing a positive or negative delay $\Delta\tau$ (with the same magnitude) between the pump and the probe, nonmirror symmetry outputs are obtained. The probe will oscillate inside the complex potential in this case, switching back and forth between regimes with positive and negative imaginary parts [29]. Figure 4(a) shows the output temporal profiles of the probe when it is launched in the fundamental mode with $\pm\Delta\tau$. As depicted, the two outputs are not a mirror symmetry of each other, unlike the inputs. The reason is due to the shock term that modifies the soliton-induced potential and transforms it from a regular symmetric one to a $\mathcal{PT}$-symmetric potential. As the imaginary part of the potential increases, this nonmirror symmetry increases, even though $\mathcal{PT}$ symmetry itself is not broken. Figure 4(b) shows the parity breaking when the probe is launched in the first-order mode.

In conclusion, we have studied the interaction between a strong soliton and a weak probe in a symmetric HC PCF filled by a noble gas in the presence of the self steepening (shock) effect. The two pulses have the same central frequency and opposite circular polarization states. The medium is Raman and plasma free. The probe is trapped during propagation because of the soliton-induced potential that always has two localized modes. We have proven theoretically that the shock term modifies the soliton-induced potential, which becomes $\mathcal{PT}$ symmetric, by introducing an odd imaginary component to the potential. We have found that the eigenvalues of the system are always real or, in other words, the $\mathcal{PT}$ symmetry is always unbroken. Finally, we have demonstrated numerically the parity-breaking property by introducing a positive or negative time delay (with the same absolute value) between the pump and the probe. We believe that our results will open different configurations and avenues for observing $\mathcal{PT}$-symmetry breaking in optical fibers, without the need to resort to complex microstructures.

We would like to thank Philip St. J. Russell for useful discussions. This research was funded by the German Max Planck Society for the Advancement of Science.

[1] L. D. Landau and E. M. Lifshitz, *Quantum Mechanics Non-Relativistic Theory*, 3rd ed. (Pergamon, Oxford, 1977).

[2] C. M. Bender and S. Boettcher, Phys. Rev. Lett. **80**, 5243 (1998).

[3] C. M. Bender, S. Boettcher, and P. N. Meisinger, J. Math. Phys. **40**, 2201 (1999).

[4] R. El-Ganainy, K. G. Makris, D. N. Christodoulides, and Z. H. Musslimani, Opt. Lett. **32**, 2632 (2007).

[5] Z. H. Musslimani, K. G. Makris, R. El-Ganainy, and D. N. Christodoulides, Phys. Rev. Lett. **100**, 030402 (2008).

[6] Z. H. Musslimani, K. G. Makris, R. El-Ganainy, and D. N. Christodoulides, J. Phys. A: Math. Theor. **41**, 244019 (2008).

[7] S. Longhi, Phys. Rev. Lett. **103**, 123601 (2009).

[8] A. A. Sukhorukov, Z. Xu, and Y. S. Kivshar, Phys. Rev. A **82**, 043818 (2010).

[9] Y. D. Chong, L. Ge, and A. D. Stone, Phys. Rev. Lett. **106**, 093902 (2011).

[10] A. Szameit, M. C. Rechtsman, O. Bahat-Treidel, and M. Segev, Phys. Rev. A **84**, 021806 (2011).

[11] S. Longhi, F. Cannata, and A. Ventura, Phys. Rev. B **84**, 235131 (2011).

[12] N. V. Alexeeva, I. V. Barashenkov, A. A. Sukhorukov, and Y. S. Kivshar, Phys. Rev. A **85**, 063837 (2012).

[13] J. Sheng, M. A. Miri, D. N. Christodoulides, and M. Xiao, Phys. Rev. A **88**, 041803 (2013).

[14] S. Klaiman, U. Günther, and N. Moiseyev, Phys. Rev. Lett. **101**, 080402 (2008).

[15] A. Guo, G. J. Salamo, D. Duchesne, R. Morandotti, M. Volatier-Ravat, V. Aimez, G. A. Siviloglou, and D. N. Christodoulides, Phys. Rev. Lett. **103**, 093902 (2009).

[16] C. E. Rüter, K. G. Makris, R. El-Ganainy, D. N. Christodoulides, M. Segev, and D. Kip, Nat. Phys. **6**, 192 (2010).

[17] A. Regensburger, C. Bersch, M. A. Miri, G. Onishchukov, D. N. Christodoulides, and U. Peschel, Nature (London) **488**, 167 (2012).

[18] P. St. J. Russell, Science **299**, 358 (2003).

[19] P. St. J. Russell, J. Lightwave Technol. **24**, 4729 (2006).

[20] J. C. Travers, W. Chang, J. Nold, N. Y. Joly, and P. St. J. Russell, J. Opt. Soc. Am. B **28**, A11 (2011).

[21] O. H. Heckl, C. R. E. Baer, C. Kränkel, S. V. Marchese, F. Schapper, M. Holler, T. Südmeyer, J. S. Robinson, J. W. G. Tisch, F. Couny, P. Light, F. Benabid, and U. Keller, Appl. Phys. B **97**, 369 (2009).

[22] N. Y. Joly, J. Nold, W. Chang, P. Hölzer, A. Nazarkin, G. K. L. Wong, F. Biancalana, and P. St. J. Russell, Phys. Rev. Lett. **106**, 203901 (2011).

[23] W. Chang, A. Nazarkin, J. C. Travers, J. Nold, P. Hölzer, N. Y. Joly, and P. St. J. Russell, Opt. Express **19**, 21018 (2011).

[24] P. Hölzer, W. Chang, J. C. Travers, A. Nazarkin, J. Nold, N. Y. Joly, M. F. Saleh, F. Biancalana, and P. St. J. Russell, Phys. Rev. Lett. **107**, 203901 (2011).

[25] M. F. Saleh, W. Chang, P. Hölzer, A. Nazarkin, J. C. Travers, N. Y. Joly, P. St. J. Russell, and F. Biancalana, Phys. Rev. Lett. **107**, 203902 (2011).

[26] M. F. Saleh and F. Biancalana, Phys. Rev. A **84**, 063838 (2011).

[27] W. Chang, P. Hölzer, J. C. Travers, and P. St. J. Russell, Opt. Lett. **38**, 2984 (2013).

[28] M. F. Saleh, W. Chang, J. C. Travers, P. St. J. Russell, and F. Biancalana, Phys. Rev. Lett. **109**, 113902 (2012).

[29] M. F. Saleh and F. Biancalana, Phys. Rev. A **87**, 043807 (2013).

[30] G. P. Agrawal, *Nonlinear Fiber Optics*, 4th ed. (Academic, San Diego, 2007).

[31] D. Anderson and M. Lisak, Phys. Rev. A **27**, 1393 (1983).

[32] Z. Wei-Ping and L. Hong-Ji, Chin. Phys. Lett. **17**, 577 (2000).

[33] S. P. Benham, J. M. Thijssen, and J. E. Inglesfield, Comput. Phys. Commun. **136**, 64 (2001).

[34] S. Fan, R. Baets, A. Petrov, Z. Yu, J. D. Joannopoulos, W. Freude, A. Melloni, M. Popović, M. Vanwolleghem, D. Jalas, M. Eich, M. Krause, H. Renner, E. Brinkmeyer, and C. R. Doerr, Science **335**, 38 (2012).

[35] D. Jalas, A. Petrov, M. Eich, W. Freude, S. Fan, Z. Yu, R. Baets, M. Popović, A. Melloni, J. D. Joannopoulos, M. Vanwolleghem, C. R. Doerr, and H. Renner, Nat. Photon. **7**, 579 (2013).